Available online at www.sciencedirect.com

SCIENCE DIRECT®

Sedimentary Geology 171 (2004) 37–58

Sedimentary Geology

www.elsevier.com/locate/sedgeo

Rutile geochemistry and its potential use in quantitative provenance studies

T. Zack[a,b,*], H. von Eynatten[c], A. Kronz[d]

[a]*Mineralogisches Institut, Universität Heidelberg, Im Neuenheimer Feld 236, 69120 Heidelberg, Germany*
[b]*Geology Department, University of Maryland, College Park, USA*
[c]*Geowissenschaftliches Zentrum der Universität Göttingen, Abteilung Sedimentologie und Umweltgeologie, Goldschmidtstrasse 3, 37077 Göttingen, Germany*
[d]*Geowissenschaftliches Zentrum der Universität Göttingen, Abteilung Geochemie, Goldschmidtstrasse 1, 37077 Göttingen, Germany*

Received 15 November 2003; received in revised form 16 March 2004; accepted 12 May 2004

Abstract

Rutile is among the most stable detrital minerals in sedimentary systems. Information contained in rutile is therefore of prime importance, especially in the study of mature sediments, where most diagnostic minerals are no longer stable. In contrast to zircon, rutile provides information about the last metamorphic cycle as rutile is not stable at greenschist facies conditions. Several known geochemical characteristics of rutile can be used to retrace provenance.

The lithology of source rocks can be determined using Nb and Cr contents in rutile, because the most important source rocks for rutile, metapelites and metabasites, imprint a distinct Nb and Cr signature in rutiles. Since Zr in rutile, coexisting with zircon and quartz, is extremely temperature dependent, this relationship can be used as a geothermometer. Metapelites always contain zircon and quartz, thus the Nb and Cr signatures of metapelites indicate rutiles that can be used for thermometry. The result is effectively a single-mineral geothermometer, which is to our knowledge the first of its kind in provenance studies. Several other trace elements are variably enriched in rutile, but the processes creating these variations are so far not understood.

In a case study, Al, Si, V, Cr, Fe, Zr, Nb and W contents in rutiles were obtained by electron microprobe from three sediment samples from Upstate New York. A Pleistocene glacial sand, whose source was granulite-facies rocks of the southern Adirondacks, has detrital rutile geochemical signatures which are consistent with the local Geology; a predominantly metapelitic source with a minor metabasitic contribution. Calculated temperatures for the metapelitic rutiles from the glacial sand are consistent with a predominantly granulite-facies source. The two other samples are from Paleozoic clastic wedges deposited in the foreland of the Taconian and Acadian orogenies. Here several geochemical patterns of detrital rutiles are comparable to rutiles derived from the Adirondacks, implying that rutiles eroded from the Taconian and Acadian orogens were

* Corresponding author.
E-mail address: tzack@min.uni-heidelberg.de (T. Zack).

0037-0738/$ - see front matter © 2004 Elsevier B.V. All rights reserved.
doi:10.1016/j.sedgeo.2004.05.009

originally derived from similar high grade gneiss terranes, like those found in the Adirondacks. The preferred tectonic scenario calls for an accretionary wedge where eroded Grenville province sediments accumulated, which were later recycled during the Taconian and Acadian orogenies.
© 2004 Elsevier B.V. All rights reserved.

Keywords: Rutile; Provenance; Geochemistry; Heavy minerals; Appalachians

1. Introduction

The extraction of information from detrital minerals for quantitative provenance studies has been thriving in recent years, mostly due to improvements in microanalytical techniques. Detrital zircon has received the most attention, because it figures prominently in providing various age informations of source rocks (U/Pb and (U–Th)/He: Rahl et al., 2003; U/Pb and fission-track: Carter and Bristow, 2003; U/Pb and Lu/Hf: Jacobsen et al., 2003). However, chemical, petrogenetic and radiometric signatures of numerous detrital minerals have been used for deciphering source area characteristics: e.g., garnet (Morton, 1987), chrome spinel (Pober and Faupl, 1988; von Eynatten, 2003), tourmaline (von Eynatten and Gaupp, 1999), amphibole (Faupl et al., 2002), white mica (von Eynatten et al., 1996; von Eynatten and Wijbrans, 2003) and epidote (Spiegel et al., 2002).

Surprisingly, little attention has been given to chemical properties of rutile in provenance studies to date (but see Götze. J., 1996; Preston et al., 1998, Preston et al., 2002) despite favourable sedimentological and geochemical characteristics. Rutile is, together with zircon and tourmaline, among the most stable heavy minerals during earth surface and diagenetic processes (Hubert, 1962; Morton and Hallsworth, 1999). As a result, rutile still contains information from its primary source area, even in extremely mature sediments and after burial to significant depth.

The majority of detrital rutile derives from medium to high grade metamorphic rocks (Force, 1980, Force, 1991) and recycled sediments. In contrast, it is virtually absent in a number of common rock types such as most igneous and low-grade metamorphic rocks (Force, 1980, Force, 1991). When it does exist in these rocks, rutile occurs as <40-μm thick needles (sagenite) within other phases formed by exsolution or alteration. Rutile has also been reported as an authigenic product (Mange and Maurer, 1992). Both authigenic rutile and sagenite are too fine-grained to produce sedimentary detritus of grain sizes coarser than coarse silt (see below). Minor, yet unquantified sources of rutile are alpine quartz veins, alkaline magmatites, pegmatites, kimberlites and porphyry copper deposits (Force, 1980, Force, 1991).

Whereas zircon generally survives the rock cycle from sedimentary to high grade metamorphic and often even magmatic processes, rutile breakdown occurs at the beginning of the greenschist facies and is newly formed at upper amphibolite facies conditions. Increasing pressure generally favours the formation of rutile, so that it is widespread at blueschist and eclogite facies conditions. In any case, detrital rutile should mostly reflect conditions of the last medium to high-grade metamorphism.

In this contribution, we first summarize recent advances on the understanding of trace element rutile geochemistry in metamorphic systems. In the second section, we present the first results of high precision electron microprobe data of detrital rutiles and outline how such data can be applied to quantitative provenance analysis.

2. Evaluation of rutile geochemistry

It is a well-known fact that rutile can contain highly charged elements (V, Cr, Fe, Al, Nb, Sn, Sb, Ta, W) up to the %-level (Deer et al., 1962; Graham and Morris, 1973; Haggerty, 1991; Deer et al., 1992; Smith and Perseil, 1997; Rice et al., 1998). These elements (together with Zr, Mo, Hf, Th and U) have been recently analysed in rutiles from several metamorphic rock types (Zack et al., in press). One result making rutile attractive for provenance studies is a

link between concentration of several trace elements in rutile and in surrounding host rock. Another result is a strong correlation between Zr contents in rutile and metamorphic peak temperature. Trace element contents in rutile therefore mirror the petrogenetic conditions of the surrounding rock, so that rutile contains important information of its source even after destruction of rock fabric by weathering and mechanical abrasion.

2.1. Nb–Cr systematics

Nb and Cr concentrations in rutile can be used to distinguish between rutile formed in metabasites and metapelites (Fig. 1). From a compilation of measured rutiles, it is evident that metacumulates are characterized by high Cr rutiles, other metamafic rocks contain rutiles with low Cr and low Nb contents, whereas metapelites contain rutiles with low Cr and high Nb.

This observed distinction can be explained by two properties of Nb and Cr. Rutile is extremely compatible for Nb compared to most metamorphic phases, so that rutile concentrates >90% of the available Nb and Ti in a given rock. Therefore, the Nb/Ti ratio of the source rock is mirrored in rutile. For example, the Nb/TiO_2 ratio of pelites from 9 to 27 (Plank and Langmuir, 1998; Barth et al., 2000) translates into a Nb content of rutile in metapelites of 900–2700 ppm. Cr, however, is not selective for most metamorphic minerals, so that Cr is more or less equally distributed between available minerals, and consequently, the Cr content in the source rock is also mirrored in rutile.

The very high contents of Nb in several felsic granulitic rutiles (Fig. 1) are not completely understood. A likely reason may be the role of high-Ti biotite. This mineral is stable up to very high temperature and could accommodate a substantial amount of the whole rock Ti in felsic and metapelitic rock types. Partition coefficients between biotite and melt indicate a strong enrichment of Ti compared to Nb (e.g., LaTourrette et al., 1995). The dominance of biotite for Ti should result in a low modal abundance of rutile, while most of the Nb will be concentrated in rutile. If the above explanation is valid, this process would not influence the behaviour of Nb in metabasites in granulite-facies rocks since biotite is never a major phase in these rocks.

2.2. Rutile thermometry

In assemblages that contain zircon, the Zr content of rutile is buffered and constant at fixed intensive parameters (pressure, temperature). With quartz as an excess phase, a reaction can be written as such:

$$ZrSiO_4(\text{zircon}) = ZrO_2(\text{in rutile}) + SiO_2(\text{quartz})$$

In metamorphic assemblages that contain zircon, rutile and quartz in equilibrium, changing temperature only changes the abundance of Zr in rutile since zircon and quartz are nearly pure phases. Following this reasoning, Zr contents in rutile have been

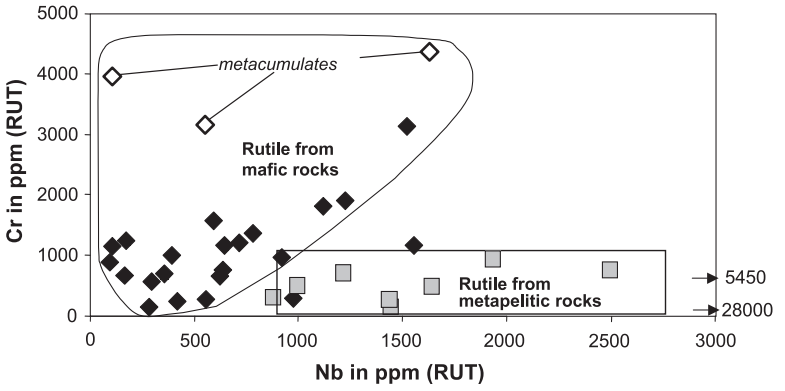

Fig. 1. Plot of Nb vs. Cr contents of rutile from different metamorphic environments (Zack et al., in press). Black diamonds—metamafic rocks; open diamonds—metamafic rocks with a cumulate protolith; grey squares—metapelitic rocks; arrows—felsic granulite-facies rocks with exceptionally high Nb content. Field for metapelitic rutiles was set between 900 and 2700 ppm Nb as explained in text.

measured by (Zack et al., in press) from metamorphic samples with different peak temperatures (from 400 to 1100 °C) that contain excess quartz and zircon. The result is a very strong positive correlation of Zr content in rutile and increasing temperature (Fig. 2). Although samples experienced pressures from 0.9 to 4.5 GPa, no pressure influence on the Zr incorporation in rutile has been found, making the "rutile thermometer" an ideal geothermometer.

Equilibrium in metamorphic systems depends on sufficient element mobility to make exchange between mineral phases possible. Increasing temperature (prograde metamorphism) generally involves the release of fluid by dehydration reactions, which enhances element mobility. In comparison, conditions of decreasing temperature (retrograde metamorphism) are often characterized by the absence of fluid, therefore preserving peak temperature mineral assemblages. In the case of rutile, Zr concentration generally records peak temperature conditions. However, reequilibration during retrograde metamorphism is possible at any lower temperature during the influx of external fluids. The extent of this process is variable even on a metre scale, but for reequilibration of Zr content in rutile, the extent is at least limited in the samples so far investigated by (Zack et al., in press).

Measurement of the Zr content in detrital rutile will give an estimate for the minimum temperature experienced by the source rock, if it can be demonstrated that zircon and quartz are excess phases. These phases are always present in metapelites. Since rutiles from such rocks are characterized by Cr content <1000 ppm and Nb between 900 and 2700 ppm, Zr content in the fraction of detrital rutiles with this specific trace element pattern can be used for deriving minimum temperature conditions of their source rock.

2.3. Other important trace element systems

A variety of trace elements are significantly incorporated in rutile (e.g., Al, V, Fe, Mo, Sn, Sb, Hf, Ta, W, Th and U). While some elements with concentrations of more than ca. 50 ppm (e.g., Al, V, Fe) can easily been analysed by electron microprobe (see below), less abundant elements can be reliably analysed by laser ablation-ICP-MS (Zack et al., 2002). Preliminary tests with the Heidelberg ion microprobe show that most of the listed trace elements can also be accurately measured (Zr, Nb, Sn, Hf, W, Th, U). Measurements of high U concentrations can assist in the selection of suitable rutile grains for several dating techniques (U/Pb: e.g., Sircombe, 1996; (U–Th)/He:

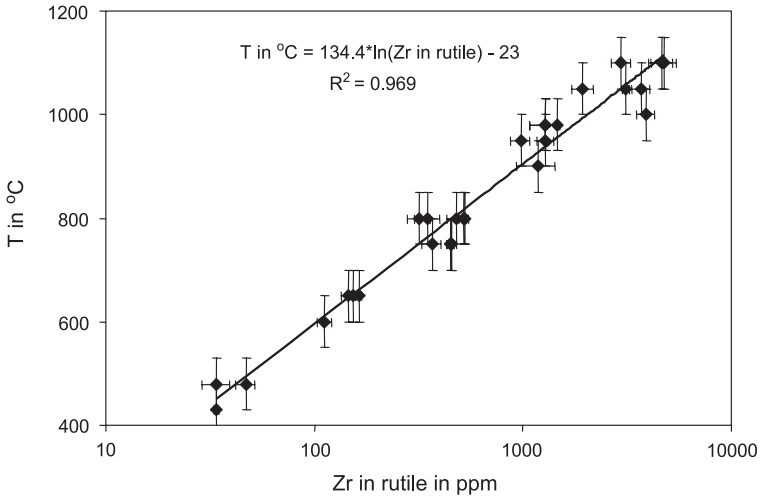

Fig. 2. Correlation of Zr content in rutile with peak metamorphic temperature based on an empirical calibration from 30 natural samples (Zack et al., in press). With increasing metamorphic grade, samples are from Samana (Dominican Republic), Syros (Greece), Confin (Switzerland), Trescolmen (Switzerland), Catalina Island (USA), Alpe Arami (Switzerland), Hengshan (China), Sneznik (Poland), Andrelandia (Brazil), Erzgebirge (Germany), Epupa (Namibia), Schwarzwald (Germany), Waldviertel (Austria), Granulitgebirge (Germany), Anapolis–Itaucu (Brazil). Temperatures are taken from published estimates for these localities. Formula for geothermometer is plotted in diagram together with the correlation coefficient.

Crowhurst et al., 2002). Applicability of these techniques can be greatly enhanced if U contents are known before analysis since different rutiles show large variations of U contents, which are often too low for dating. High concentrations of >10000 ppm of V, Nb, Sn, Sb and/or W are characteristic for rutiles related to mineral deposits, while >10000 ppm of Cr and/or Nb (up to 21 wt.% Nb_2O_5 and 7 wt.% Cr_2O_3) are typical for rutiles from kimberlitic sources (see discussion in the work of Zack et al., 2002). The systematics of Fe are so far not well understood. It has been ascribed to charge balance high-valency elements as Fe^{2+} and Fe^{3+} together with vacancies (Rice et al., 1998; Zack et al., 2002). However, we note that metamorphic rutiles contain mostly >1000 ppm Fe (Zack et al., in press).

Distributions of elements in rutile are by no means extensively investigated and through further investigations more systematics in rutiles from such environments are likely to be detected. Although several petrogenetic processes for incorporation of trace elements in rutile are not fully understood, increasing the number of variables may in any case be helpful for discrimination purposes.

3. Application to sediments of upstate New York

In order to evaluate the use of detrital rutiles in provenance studies, we investigated arenites from the same localities already studied for provenance of detrital zircon by McLennan et al. (2001). All samples (Poughquag Quartzite, Austin Glen Member, Shawangunk Formation, Catskill red bed) were found to contain rutile. Samples from the Shawangunk Formation (Lower Silurian, UNY 7, Fig. 3) and Catskill red bed (Upper Devonian, UNY 13, Fig. 3) were chosen for detailed microprobe analysis for representing different sedimentary and diagenetic environments. The Shawangunk sample might have been influenced by hydrothermal fluids (Kesler et al., 1997). The Catskill redbed was deposited in a subaerial environment under highly oxidising conditions. In such samples, provenance information can potentially only be derived from the most stable minerals.

Additionally, one glacial sand sample from a sand pit 1 km southwest of Gloversville (UNY 22, Fig. 3) was investigated in detail. The sand deposit originates from a subaqueous fan in front of a recessional moraine during the waning stages of the last ice age (Dineen and Hanson, 1995). The glacier originated from the Adirondack highlands and flowed down along the Sacandaga valley. Underlying rock types of this glacier were therefore predominantly high grade metamorphic rocks (mostly granulite-facies rocks; e.g., Bohlen et al., 1985).

3.1. Analytical method

Samples UNY 7 and UNY 13 were carefully crushed and all samples subsequently sieved into 63–125 and 125–250 μm grain-size fractions. Heavy minerals were separated using centrifuge-aided settling in sodium–metatungstate (calibrated density 2.88 ± 0.02 g/cm^3). Rutile from each sample and each grain-size fraction was then further concentrated by magnetic separation. The remaining non-magnetic to slightly magnetic fractions were embedded in epoxy resin and polished for electron microprobe analysis (see below). Before magnetic separation, a small part of the heavy mineral fraction of the 63–125 μm grain-size fractions was mounted on a slide for microscopic investigation of heavy mineral associations. About 100 non-opaque grains were counted using the ribbon-counting method (Mange and Maurer, 1992) to estimate relative frequencies of individual heavy mineral phases. In addition, we calculated the weight-percentage of the heavy mineral fraction relative to the whole sample and the ratio of non-opaque to opaque grains in heavy mineral slides in order to estimate the overall rutile content of the samples, at least for the 63–125 μm grain-size fraction.

All analyses were conducted with a JEOL JXA 8900RL electron microprobe at Universität Göttingen and University of Maryland as described by Zack et al. (2002). Acceleration voltage was set at 20 kV, beam current at 120 nA and beam diameter at 5 μm. Counting time on the peak was set at 15 s for Ti, 60 s for Si, 150 s for Cr, Fe and V, 250 s for Al and 300 s for Nb and Zr, resulting in an analysis time for each spot of 12 min. A PETJ spectrometer was chosen for Zr due to its highest sensitivity for this element. Every 10 analyses of unknown rutiles were bracketed by two synthetic rutiles for zero-concentration count rates on the peaks and to exclude any machine drift. Calculated detection limits were 15

ppm for Al, 30 ppm for Si, 60 ppm for V, 40 ppm for Cr, 35 ppm for Fe, 30 ppm for Zr, 50 ppm for Nb and 120 ppm for W.

Several rutiles, especially those from the Catskill and Shawangunk samples, show signs of beginning breakdown probably related to diagenetic processes. A sequence of increasing alteration is depicted in Fig. 4. While rutile in Fig. 4a shows no sign of alteration, rutiles in Fig. 4b and c have numerous small cracks partly filled by iron-rich oxides and/or hydroxides. Such areas could sometimes not be avoided during analysis and all measurements with Fe >30000 ppm were treated as being influenced by alteration and excluded from further analysis. Otherwise, systematic zonations were not observed by back-scattered imaging, thus only one analysis per grain was made.

3.2. Description of samples

Shawangunk (sample UNY 7): a mature pebbly quartz arenite of Lower Silurian age, contains 0.2% heavy minerals in the 63–125 μm grain-size fraction with about one-third being translucent. This rock is characterized by a very stable association with ZTR (zircon+tourmaline+rutile; Hubert, 1962) being close to 100%. Zircon predominates (63%) and is followed by tourmaline (28%) and rutile (7%). The zircon/rutile ratio therefore is 9.0 (n=70). Rare accessory minerals observed are kyanite and titanite.

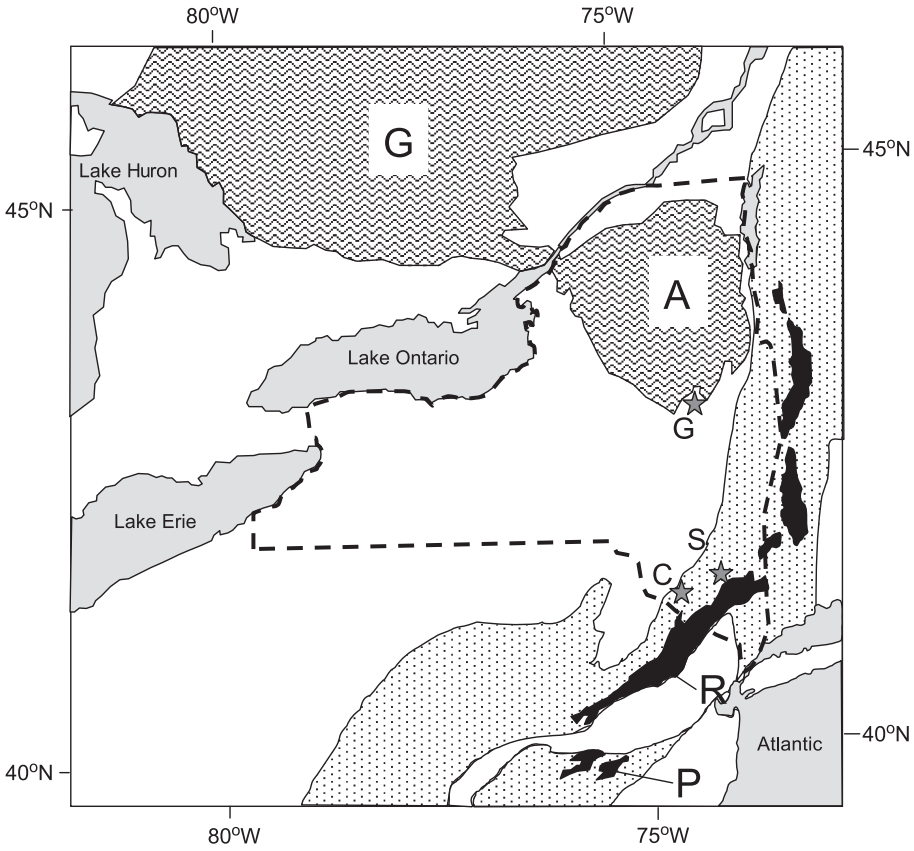

Fig. 3. Schematic geological map of Upstate New York (stippled outline) and surrounding areas. Wavy-Middle Proterozoic high grade rocks without later metamorphic overprint (A—Adirondacks, G—Grenville), black—Middle Proterozoic high grade rocks with Taconic and Acadian metamorphic overprint (P—West Chester Dome, Piedmont; R—Reading Prong), dotted—Paleozoic rocks deformed during Taconian and Acadian orogenies (S—locality of Shawangunk sample, UNY 7; C—locality of Catskill sample, UNY 13), white—other rocks, e.g., Archean, undeformed Paleozoic, Mesozoic, Quaternary (G—locality of Gloversville sample, UNY 22).

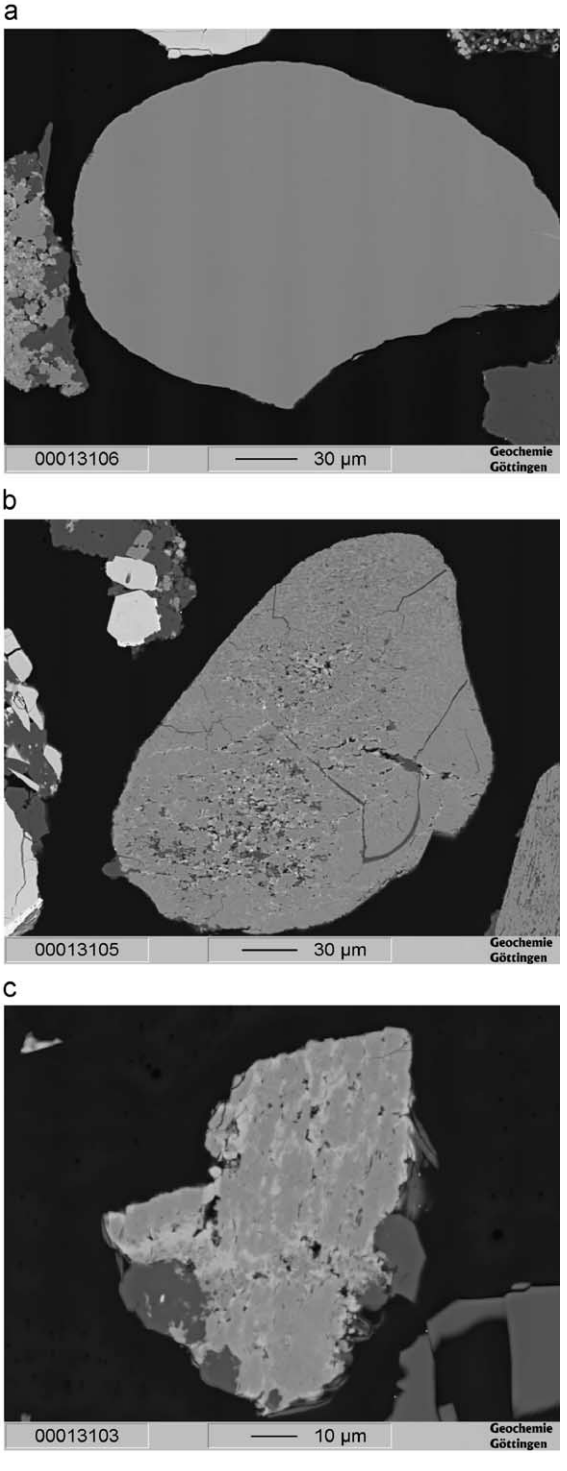

Fig. 4. Back scattered images of detrital rutiles from Shawangunk sample showing different degrees of alteration. (a) Pristine detrital grain of rutile with no signs of alteration. (b) Detrital rutile with beginning alteration. Parts of the grain are replaced by iron-rich oxides/hydroxides (white) and quartz (dark grey). Rutile still shows well-rounded grain shape and some areas of the rutile are chemically unaltered. (c) Detrital grain with strong alteration. Whole grain is pervasively riddled with iron-rich oxides/hydroxides (white), remaining rutile is chemically enriched in Fe and surface shows dissolution features.

Catskill (sample UNY 13): a redbed sandstone of Upper Devonian age, contains 2.2% heavy minerals but a very low ratio of non-opaque to opaque grains of about 1:20, so that the absolute amount of translucent heavy mineral is comparable to sample UNY 7. Also quite similar is the high amount of ZTR with zircon predominance (60%) followed by tourmaline (21%) and rutile (7%), but apatite is present in this sample (7%) and accessory minerals are kyanite, amphibole, chlorite, and brookite/anatase. This translates into a zircon/rutile ratio of 8.6 (n=67).

Gloversville (sample UNY 22): a glacial sand containing a very high percentage of heavy minerals (11.4% in the 63–125 µm grain-size fraction), and a high ratio of non-opaque to opaque grains of about 6:1. Consequently, almost 10% of the sample comprises translucent heavy minerals. Accordingly, the heavy mineral association is extremely immature with ZTR being less than 10%. The vast majority of heavy minerals is constituted by pyroxene (~50%) and garnet (~40%). Minor contributions come from zircon, tourmaline, rutile, apatite and amphibole. Counting only for zircon and rutile grains, the zircon/rutile ratio is found to be 3.1 (n=58).

3.3. Results

Detrital rutiles from all three investigated samples show a large variation in composition that has not been reported to date. (Nb <50 to 19930 ppm, Cr <40 to 3314 ppm, Zr <30 to 3891 ppm, Fe <35 to 30,000 ppm (see above), V <60 to 7576 ppm, W <120 to 8067 ppm; Fig. 5, Tables 1–3). The histogram patterns (Fig. 5) of all three samples show some overall similarities. They all have a maximum distribution of Cr contents in the range 0–200 ppm, with higher Cr contents rapidly decreasing in abundance (Fig. 5a).

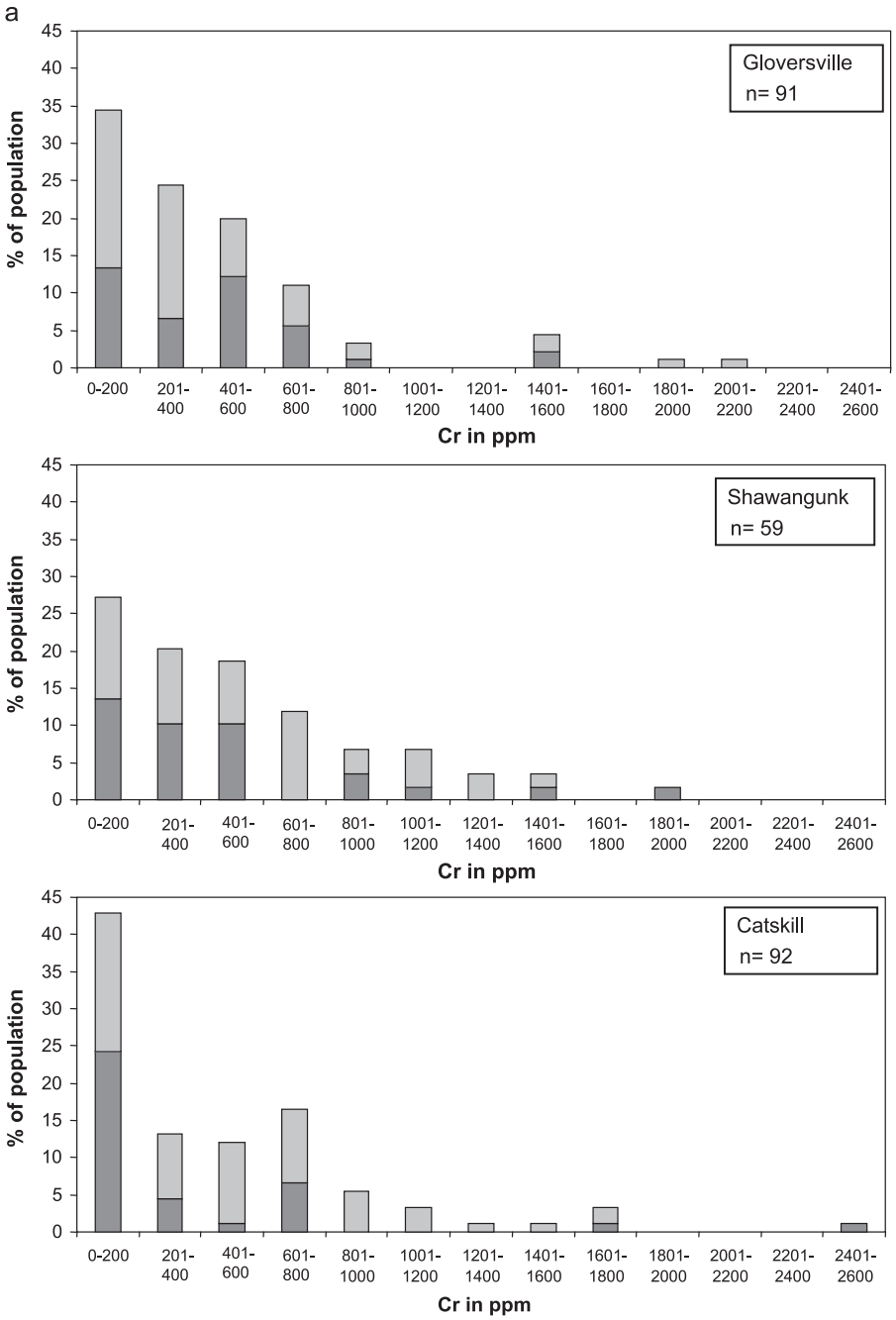

Fig. 5. Histograms of (a) Cr, (b) Nb, (c) Zr and (d) Fe content of rutile for Gloversville, Shawangunk and Catskill samples. Abundance in % of whole population. Dark grey: 63–125 μm size fraction, light grey: 125–250 μm size fraction. Hatched fields in (c) are rutiles that do not fall in the field of metapelitic rutiles. Hatched rutiles are also subdivided in 63–125 μm and 125–250 μm size fractions (dark and light grey, respectively). Metapelitic rutiles in (c) (filled dark and light grey) are used for Fig. 6.

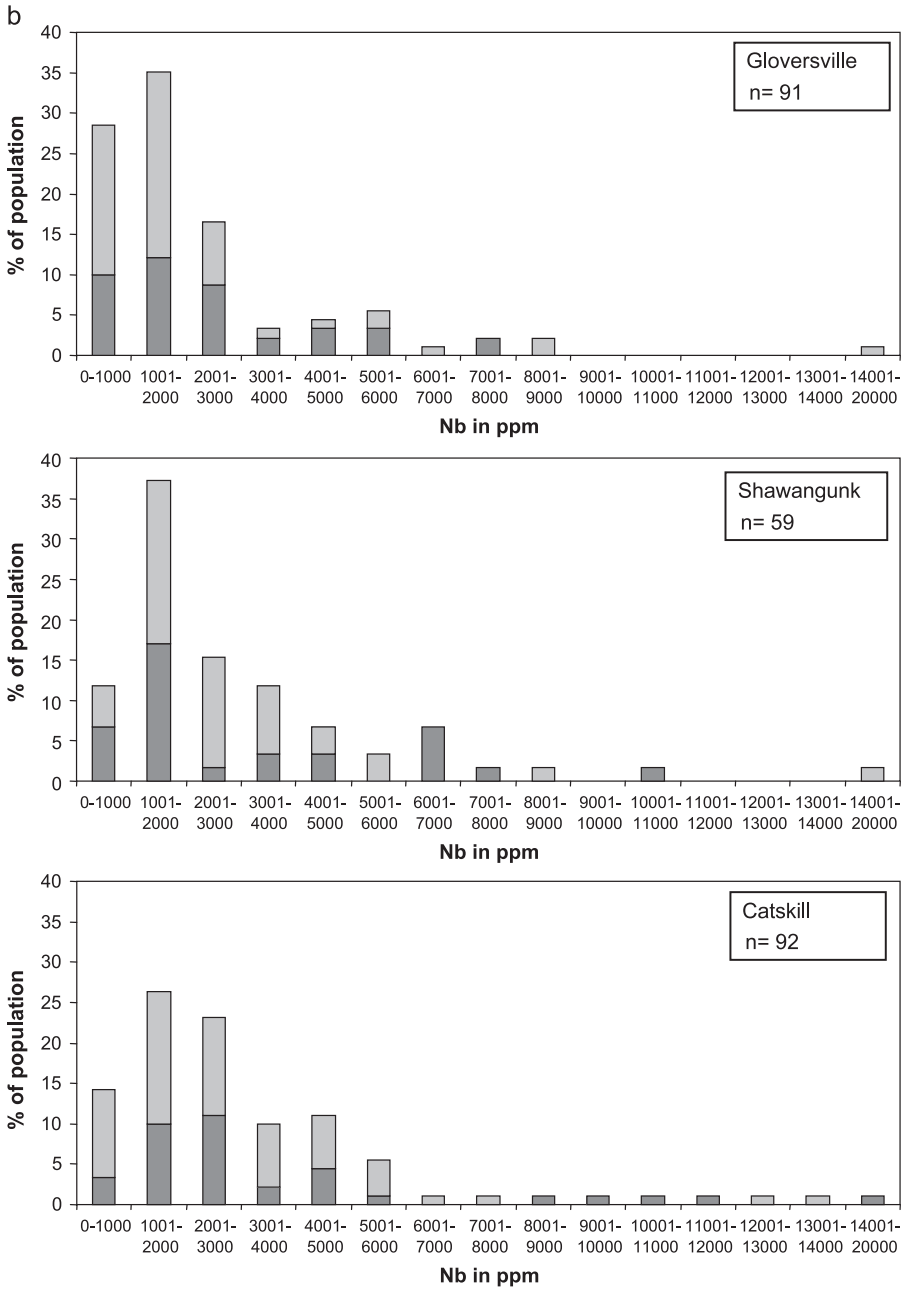

Fig. 5 (*continued*).

All three samples also have the same maximum peak in the interval 1000–2000 ppm for Nb and a tailing end towards very high values (15,000–20,000 ppm; Fig. 5b). The Zr patterns of all three samples show a pronounced peak at 0–200 ppm, followed by a strong drop at 200–400 ppm and then a second more diffuse maximum between 400 and 1200 ppm (Fig. 5c). There is no apparent difference in composition between the two different grain size fractions, although this may be due to insufficient number of

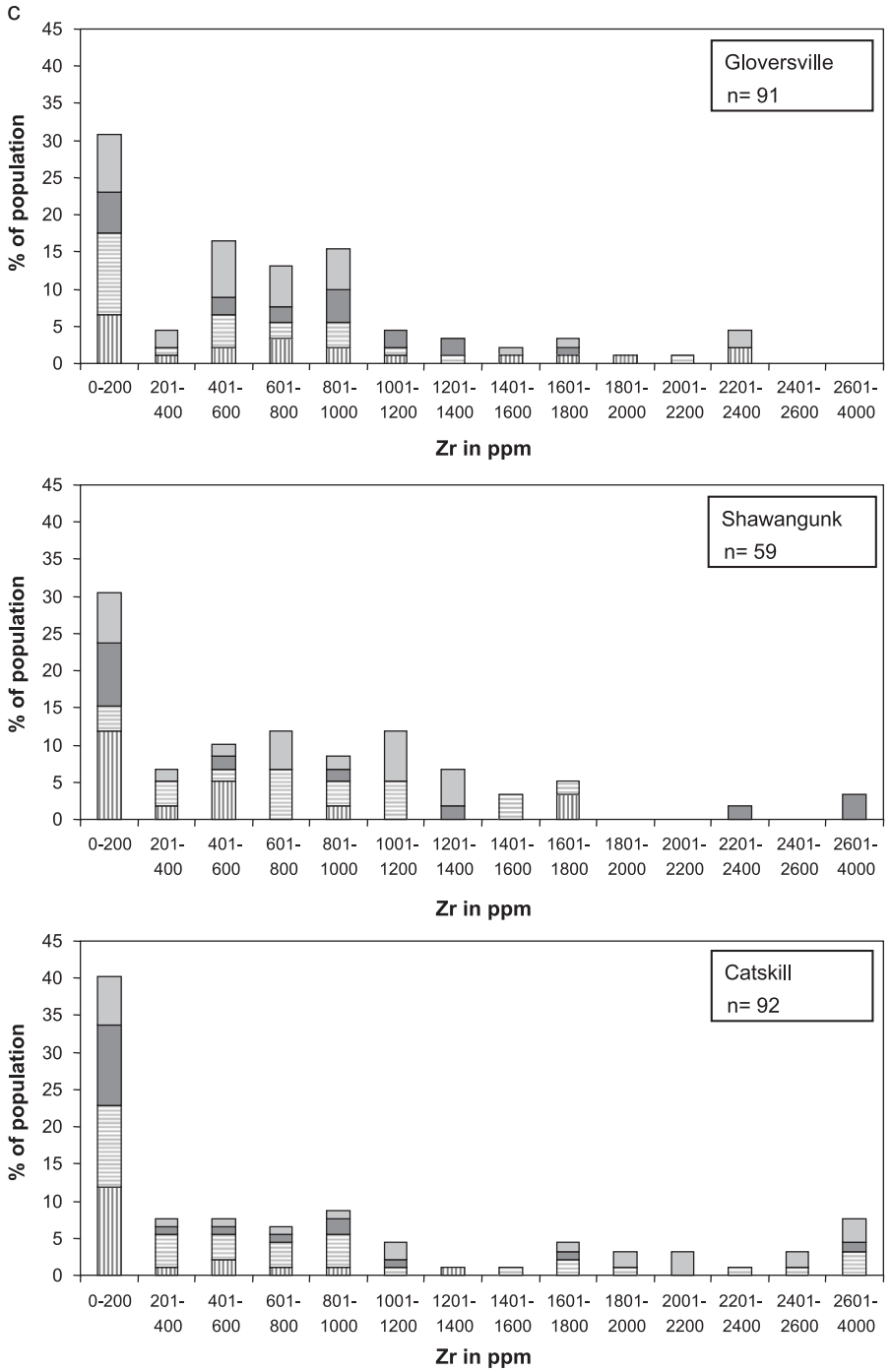

Fig. 5 (*continued*).

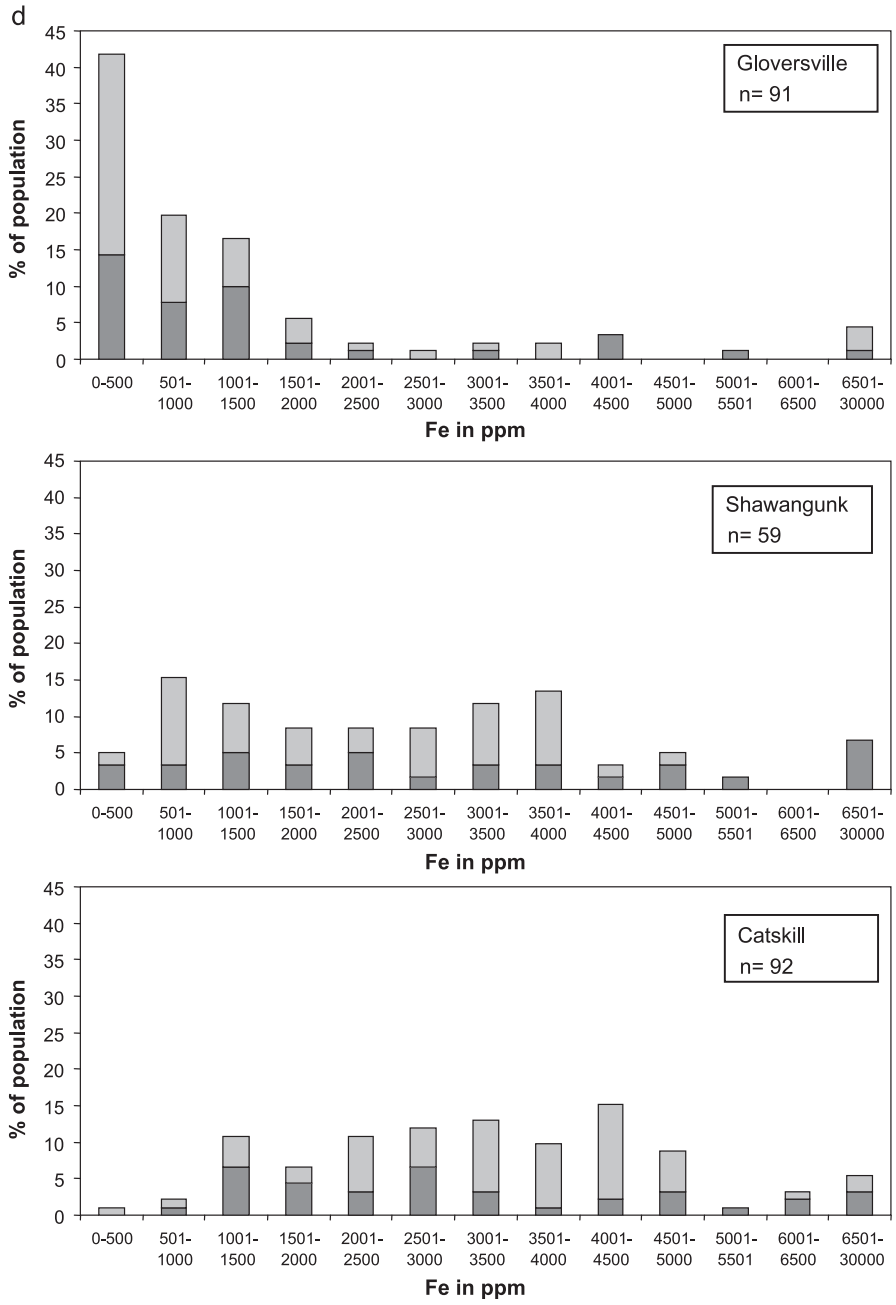

Fig. 5 (*continued*).

analysed grains in each fraction. An exception might be found in distribution of Zr contents in Shawangunk and Catskill samples (see next discussion).

Temperatures of the rutile-bearing source rocks were calculated for "metapelitic rutiles" (Cr <1000 ppm, Nb 900–2700 ppm) by using their Zr contents as

Table 1
Electron microprobe data for detrital rutile in ppm

Grain #	Al	Si	V	Cr	Fe	Zr	Nb	W
125–250 μm grain-size fraction								
200	38	745	60	b.d.	2299	b.d.	b.d.	b.d.
201	113	734	487	0	3051	235	2445	b.d.
202	b.d.	b.d.	3002	107	55	182	991	b.d.
203	72	173	851	b.d.	254	b.d.	514	b.d.
204	25	112	b.d.	b.d.	456	150	5158	b.d.
205	244	b.d.	1678	341	1886	512	5164	410
206	45	b.d.	2063	389	697	650	475	b.d.
207	98	678	74	b.d.	3903	b.d.	2746	124
208	36	b.d.	1418	307	1130	421	1389	b.d.
209	b.d.	b.d.	2646	158	105	988	478	b.d.
210	77	b.d.	1836	510	1859	1064	4897	225
211	b.d.	b.d.	5232	1486	178	2018	1756	b.d.
212	b.d.	b.d.	4137	211	695	1437	1142	b.d.
213	82	b.d.	1530	999	660	649	1182	b.d.
214	101	b.d.	1697	360	1282	787	1703	228
215	129	b.d.	1742	242	1023	2236	1651	b.d.
216	b.d.	97	729	b.d.	471	b.d.	1668	b.d.
217	173	515	84	b.d.	11,946	104	15,178	b.d.
218	368	257	137	b.d.	6796	b.d.	3536	b.d.
219	46	b.d.	1290	123	1007	767	588	124
223	b.d.	b.d.	4264	627	152	829	488	b.d.
224	90	b.d.	2863	592	601	2229	2143	425
225	b.d.	b.d.	5120	622	91	1698	1093	147
226	26	b.d.	1899	342	467	558	1317	b.d.
228	257	172	4082	1598	283	b.d.	2747	b.d.
229	103	513	75	b.d.	523	110	757	b.d.
230	111	36	4432	81	161	74	930	b.d.
231	b.d.	57	65	b.d.	1251	28	2184	b.d.
232	21	b.d.	4783	893	121	601	1622	b.d.
233	36	107	68	b.d.	6409	33	8052	b.d.
234	30	b.d.	3345	248	218	530	2712	b.d.
235	897	390	462	158	528	b.d.	961	b.d.
236	30	217	b.d.	b.d.	1650	b.d.	236	b.d.
237	240	b.d.	2497	570	2500	889	8303	127
238	24	b.d.	2136	b.d.	91	b.d.	1013	b.d.
239	b.d.	b.d.	1566	400	746	536	1932	b.d.
240	b.d.	32	2561	392	324	986	754	b.d.
241	26	144	b.d.	b.d.	512	44	428	b.d.
250	n.a.	n.a.	n.a.	495	269	1239	366	b.d.
251	n.a.	n.a.	n.a.	1866	3965	468	6960	612
252	n.a.	n.a.	n.a.	221	429	436	220	b.d.
253	n.a.	n.a.	n.a.	541	442	487	1332	215
254	n.a.	n.a.	n.a.	365	668	771	1419	b.d.
255	n.a.	n.a.	n.a.	2066	63	312	998	1375
256	n.a.	n.a.	n.a.	243	200	362	1533	b.d.
257	n.a.	n.a.	n.a.	647	789	584	1055	b.d.
258	n.a.	n.a.	n.a.	242	b.d.	888	1155	b.d.
259	n.a.	n.a.	n.a.	298	597	933	772	b.d.
260	n.a.	n.a.	n.a.	610	442	881	1440	538
261	n.a.	n.a.	n.a.	634	489	894	1419	507
262	n.a.	n.a.	n.a.	485	123	492	1376	b.d.
263	n.a.	n.a.	n.a.	550	21	497	1025	b.d.

Table 1 (*continued*)

Grain #	Al	Si	V	Cr	Fe	Zr	Nb	W
125–250 μm grain-size fraction								
264	n.a.	n.a.	n.a.	372	1068	643	2686	b.d.
63–125 μm grain-size fraction								
156	238	b.d.	992	633	1024	433	1343	123
157	95	b.d.	2355	618	1164	584	2415	142
158	b.d.	50	b.d.	b.d.	1061	b.d.	601	b.d.
159	27	b.d.	2681	298	312	667	1545	168
160	27	36	b.d.	b.d.	472	272	5316	b.d.
161	49	126	291	108	238	b.d.	1990	b.d.
162	270	b.d.	869	194	4310	720	5536	217
163	163	b.d.	1749	449	1860	862	4117	b.d.
164	152	b.d.	1457	679	1417	513	4136	1016
165	228	281	211	0	27,638	126	2068	452
166	109	b.d.	742	242	2025	650	3268	b.d.
167	b.d.	b.d.	3918	574	96	1641	411	b.d.
168	b.d.	b.d.	7146	598	b.d.	2312	441	b.d.
169	b.d.	b.d.	7145	612	b.d.	2381	464	b.d.
171	21	b.d.	4917	588	126	729	2643	b.d.
172	816	111	1609	262	528	b.d.	1650	b.d.
173	174	b.d.	834	87	1386	541	2964	b.d.
174	41	b.d.	1974	409	1196	1807	2842	330
175	82	b.d.	2021	553	772	870	2124	326
178	439	693	1348	b.d.	1024	49	807	b.d.
179	68	627	b.d.	b.d.	4411	46	2599	204
180	318	b.d.	2669	601	1205	949	3015	716
181	48	57	142	b.d.	370	847	1319	b.d.
182	291	b.d.	1337	400	4340	1002	7573	890
183	44	188	142	b.d.	3482	31	95	b.d.
184	b.d.	b.d.	3113	423	b.d.	809	1504	b.d.
185	b.d.	b.d.	939	289	633	33	898	b.d.
186	292	480	3685	1408	209	b.d.	1161	b.d.
187	b.d.	b.d.	3289	1486	b.d.	47	620	b.d.
188	b.d.	b.d.	2666	3314	1096	639	7190	b.d.
189	b.d.	b.d.	4117	592	48	1758	824	b.d.
190	62	b.d.	1632	186	745	1227	1261	b.d.
191	77	b.d.	1980	414	915	807	1466	b.d.
193	31	b.d.	932	982	1597	1415	4030	b.d.
194	b.d.	b.d.	1670	308	972	1224	1656	b.d.
195	b.d.	b.d.	2560	366	555	1073	1188	b.d.
196	65	b.d.	2755	595	494	1137	2023	133
197	63	58	103	b.d.	5082	28	5468	186

Gloversville glacial sand (UNY 22).
b.d.–below detection limit, n.a.–not analysed.

a measure of peak temperature for each single rutile. A broad similarity of the three samples is again apparent when plotting the results in a histogram (Fig. 6). While very few rutiles record amphibolite/eclogite-facies conditions, all samples show a more or less pronounced peak at greenschist/blueschist-facies temperatures and are characterized by a majority of granulite-facies rutiles. We note that even the highest calculated temperature (1046 °C) does not exceed the limit of known granulite-facies rocks (>1100 °C; Harley, 1989), giving further support for the new rutile thermometer. Calculated temperatures for the Catskill sample might be dependent on grain size. While the finer grain-size fraction has mostly tempe-

Table 2
Electron microprobe data for detrital rutile in ppm

Grain #	Al	Si	V	Cr	Fe	Zr	Nb	W
125–250 μm grain-size fraction								
51	b.d.	b.d.	843	776	3790	1114	3291	139
52	16	b.d.	2377	675	3802	751	1889	b.d.
54	106	445	b.d.	b.d.	984	27	1467	139
56	b.d.	b.d.	3094	902	4294	1063	1758	340
57	b.d.	b.d.	125	b.d.	1353	182	1386	b.d.
58	408	912	81	110	3017	399	2136	366
66	143	b.d.	726	72	2925	87	865	165
67	b.d.	b.d.	5937	749	1373	779	8930	1302
68	b.d.	b.d.	1723	370	3314	848	2869	234
70	91	b.d.	b.d.	b.d.	3989	b.d.	1154	b.d.
74	b.d.	b.d.	1857	251	420	499	1726	b.d.
76	b.d.	b.d.	5300	1068	1796	1570	2891	295
81	b.d.	b.d.	184	b.d.	3646	640	5336	122
82	b.d.	b.d.	1468	1240	2769	1096	3774	b.d.
265	n.a.	n.a.	n.a.	388	3514	1053	1216	b.d.
266	n.a.	n.a.	n.a.	558	3313	1158	1510	b.d.
267	n.a.	n.a.	n.a.	646	1044	1621	3057	b.d.
268	n.a.	n.a.	n.a.	1148	4846	1187	19,930	249
269	n.a.	n.a.	n.a.	436	918	1269	1669	b.d.
270	n.a.	n.a.	n.a.	510	2468	1188	2254	b.d.
271	n.a.	n.a.	n.a.	71	1988	158	132	b.d.
272	n.a.	n.a.	n.a.	729	2724	492	4270	177
273	n.a.	n.a.	n.a.	1575	1524	904	5363	b.d.
274	n.a.	n.a.	n.a.	921	3920	750	3738	1100
275	n.a.	n.a.	n.a.	353	565	1225	1671	b.d.
276	n.a.	n.a.	n.a.	648	3318	151	2837	b.d.
277	n.a.	n.a.	n.a.	559	3394	1257	1573	b.d.
278	n.a.	n.a.	n.a.	621	1147	1583	3050	b.d.
279	n.a.	n.a.	n.a.	b.d.	2041	252	2917	b.d.
280	n.a.	n.a.	n.a.	1000	518	763	2365	233
281	n.a.	n.a.	n.a.	429	2675	959	834	b.d.
282	n.a.	n.a.	n.a.	348	946	769	1932	b.d.
283	n.a.	n.a.	n.a.	347	979	728	2753	b.d.
284	n.a.	n.a.	n.a.	1300	516	221	4369	b.d.
63–125 μm grain-size fraction								
3	b.d.	b.d.	4914	971	1165	1669	6886	b.d.
4	b.d.	b.d.	4946	930	1213	1721	6945	b.d.
6	b.d.	b.d.	1827	407	3393	815	6559	b.d.
7	b.d.	54	1750	401	1892	2271	1815	b.d.
8	b.d.	b.d.	1230	305	1322	903	1070	115
10	42	b.d.	340	522	6329	495	6442	261
11	97	50	b.d.	b.d.	3434	553	4874	150
14	60	235	324	b.d.	5249	15	63	b.d.
15	56	91	b.d.	250	2119	156	4602	156
17	102	47	624	105	1815	133	1172	b.d.
21	b.d.	b.d.	1475	189	2615	3891	2223	b.d.
22	29	254	1179	157	4146	41	47	b.d.
23	38	76	531	284	6744	524	3739	612
26	60	b.d.	2027	557	6473	371	10,719	2932
28	b.d.	150	b.d.	1478	202	27	920	b.d.
29	b.d.	202	b.d.	1965	397	b.d.	1438	b.d.

Table 2 (*continued*)

Grain #	Al	Si	V	Cr	Fe	Zr	Nb	W
63–125 μm grain-size fraction								
32	b.d.	110	b.d.	b.d.	615	47	1397	b.d.
33	25	b.d.	2358	306	3953	3045	1181	b.d.
34	b.d.	343	b.d.	b.d.	4608	40	1297	b.d.
38	248	688	345	b.d.	2358	422	997	b.d.
39	23	b.d.	4600	587	2036	1351	1324	b.d.
40	18	b.d.	1365	478	3997	134	7579	b.d.
42	b.d.	36	3659	334	793	73	1009	b.d.
44	169	886	330	278	4553	b.d.	1163	b.d.

Shawangunk pebbly arenite (UNY 7).
b.d.–below detectffion limit, n.a.–not analysed.

ratures below 450 °C (below detection limit), the coarser grain-size fraction records a high percentage of granulite-facies rutiles.

The clearest distinction between the three samples can be found in the Fe pattern (Fig. 5d). While Catskill and Shawangunk samples show an almost uniform distribution of Fe contents between 500 and 6000 ppm, the Gloversville sample has a pronounced peak for Fe between 0 and 1500 ppm. We note that a rutile population with Fe contents <1000 ppm finds no correspondence in metamorphic rutiles analysed so far (Zack et al., in press). With statistical means, all three samples can be distinguished in terms of their rutile composition. Averages of rutile trace element compositions for each sample were plotted in different ternary diagrams (see Fig. 7 for details). In a Zr–Fe–Nb diagram, the geometric mean of sample UNY 22 can be clearly separated from samples UNY 7 and UNY 13 at a 95% confidence level, mostly due to a large fraction of rutiles with low Fe contents in sample UNY 22. In a Zr–Cr–Nb plot, sample UNY 13 can be distinguished from the other samples at a 80% confidence level, attributed to a slightly higher Nb content of the fine-grained fraction.

3.4. Comparison with regional Geology

As all three samples show broadly similar results, it is instructive to start with the glacial sand sample from Gloversville, as their source rocks can be confined to a distinct geographical area, the southern Adirondacks. Rocks in this area were subjected to granulite-facies conditions and are mostly metapelitic gneisses, felsic gneisses, charnockites and anorthosites (Bohlen et al., 1985). Only about 10% of the area contains metamafic rock types, and non-metamorphosed granites are virtually absent. The Geology of the southern Adirondacks is mirrored in the heavy mineral fraction of the glacial sand sample, which is dominated by high-grade metamorphic minerals (e.g., garnet, clinopyroxene, amphibole).

In particular, the Adirondacks Geology can be seen in the rutile geochemistry of the glacial sand. 50% of all analysed detrital rutiles fall in the field of metapelites on the basis of Nb and Cr contents, with only 20% having metamafic composition. The remaining 30% have Nb content between 2700 and 14000 ppm and may resemble felsic granulites. Seventy percent of metapelitic rutiles have granulite-facies temperatures (Fig. 6) and it is likely that rutiles with temperatures below 750 °C also originated at granulite-facies conditions, but were subjected to retrograde metamorphism. 65% of all granulite-facies rutiles fall in the range between 750 and 850 °C, mostly higher than the 675–775 °C of the classical study of Bohlen et al. (1985) about the metamorphic history of the Adirondacks. However, more recent studies found temperatures comparable with our results (820–850 °C; Spear and Markussen, 1997; Pattison et al., 2003). A maximum temperature of 976 °C calculated from detrital rutile is consistent with some Adirondacks granulites in direct contact with anorthosites in the study of Alcock and Muller (1999). Calculated temperatures in granulite-facies rocks are often lower than actual peak metamorphic conditions due to diffusional resetting during cooling (as discussed for Adirondacks granulites by Pattison et al., 2003). As emphasized by Zack et al. (in press),

Table 3
Electron microprobe data for detrital rutile in ppm

Grain #	Al	Si	V	Cr	Fe	Zr	Nb	W
125–250 μm grain-size fraction								
136	256	565	1461	354	4137	b.d.	3994	b.d.
137	191	356	1347	358	3755	b.d.	3083	b.d.
139	b.d.	b.d.	7573	645	3142	944	3185	b.d.
140	37	156	124	87	2958	805	1055	b.d.
141	303	713	1217	b.d.	4285	44	4292	242
143	162	236	483	b.d.	2171	405	3082	247
144	307	932	b.d.	b.d.	2415	b.d.	355	b.d.
146	82	212	404	b.d.	5534	79	12,697	303
147	b.d.	b.d.	2114	639	4957	2622	2051	b.d.
148	31	b.d.	65	b.d.	3956	105	4604	b.d.
149	33	43	63	b.d.	4132	171	4413	b.d.
150	260	305	345	58	4428	180	1825	b.d.
151	167	609	259	83	11,798	b.d.	13,880	617
152	19	235	b.d.	b.d.	4869	181	5580	b.d.
285	n.a.	n.a.	n.a.	1182	2018	856	1183	b.d.
286	n.a.	n.a.	n.a.	789	4957	925	4505	b.d.
287	n.a.	n.a.	n.a.	555	4288	2821	2746	b.d.
288	n.a.	n.a.	n.a.	209	1792	1164	2215	b.d.
289	n.a.	n.a.	n.a.	731	809	44	1280	b.d.
290	n.a.	n.a.	n.a.	432	3558	1743	785	b.d.
291	n.a.	n.a.	n.a.	796	1518	2758	2402	b.d.
292	n.a.	n.a.	n.a.	644	4254	2811	1653	b.d.
293	n.a.	n.a.	n.a.	356	1378	2090	1181	b.d.
294	n.a.	n.a.	n.a.	b.d.	4679	219	5028	40
295	n.a.	n.a.	n.a.	1043	3770	406	1826	b.d.
296	n.a.	n.a.	n.a.	347	2490	481	1901	113
297	n.a.	n.a.	n.a.	49	2855	683	1156	21
298	n.a.	n.a.	n.a.	88	3652	231	772	681
299	n.a.	n.a.	n.a.	522	2643	1981	1966	b.d.
300	n.a.	n.a.	n.a.	1614	1211	2673	849	b.d.
301	n.a.	n.a.	n.a.	2618	216	842	2856	620
302	n.a.	n.a.	n.a.	552	3457	1065	1902	67
303	n.a.	n.a.	n.a.	b.d.	2970	b.d.	740	b.d.
304	n.a.	n.a.	n.a.	558	4918	388	7029	881
305	n.a.	n.a.	n.a.	1136	4024	2468	2486	b.d.
306	n.a.	n.a.	n.a.	981	3245	1125	3250	b.d.
307	n.a.	n.a.	n.a.	829	3032	1983	1671	b.d.
308	n.a.	n.a.	n.a.	99	3216	b.d.	2628	687
309	n.a.	n.a.	n.a.	679	2026	695	5077	b.d.
310	n.a.	n.a.	n.a.	276	4084	45	5048	771
311	n.a.	n.a.	n.a.	1615	1436	1480	282	b.d.
312	n.a.	n.a.	n.a.	b.d.	4137	2410	828	b.d.
313	n.a.	n.a.	n.a.	743	3391	631	3501	196
314	n.a.	n.a.	n.a.	580	3124	2460	1295	b.d.
315	n.a.	n.a.	n.a.	215	4222	272	663	162
316	n.a.	n.a.	n.a.	525	3209	2901	698	b.d.
317	n.a.	n.a.	n.a.	411	3895	2189	1026	b.d.
318	n.a.	n.a.	n.a.	1516	2180	1790	2099	b.d.
319	n.a.	n.a.	n.a.	b.d.	1264	566	4752	b.d.
320	n.a.	n.a.	n.a.	546	4054	627	2793	b.d.
321	n.a.	n.a.	n.a.	891	3884	b.d.	2059	b.d.
322	n.a.	n.a.	n.a.	904	2696	2158	2572	b.d.

Table 3 (*continued*)

Grain #	Al	Si	V	Cr	Fe	Zr	Nb	W
125–250 μm grain-size fraction								
324	n.a.	n.a.	n.a.	1226	3333	2397	3037	b.d.
325	n.a.	n.a.	n.a.	972	3778	1828	4477	b.d.
326	n.a.	n.a.	n.a.	670	2194	338	135	b.d.
327	n.a.	n.a.	n.a.	203	6031	88	1519	8067
63–125 μm grain-size fraction								
86	39	87	7576	2518	5809	284	19,885	b.d.
87	b.d.	86	3026	788	1570	1038	2180	204
88	23	124	b.d.	b.d.	1129	129	2278	b.d.
89	85	246	122	58	2587	b.d.	1534	b.d.
90	991	363	232	b.d.	2822	b.d.	1465	121
91	51	85	343	58	3196	875	1547	b.d.
92	b.d.	b.d.	5661	310	2748	947	2397	1868
93	1942	713	137	b.d.	2317	b.d.	762	b.d.
94	b.d.	b.d.	893	391	3046	3043	2022	b.d.
95	b.d.	51	b.d.	b.d.	1834	67	3833	b.d.
98	138	250	b.d.	b.d.	9222	61	10821	116
99	18	b.d.	342	207	4838	b.d.	2549	b.d.
100	67	156	b.d.	b.d.	2193	73	4427	b.d.
101	27	87	2699	785	1295	502	2116	b.d.
103	41	b.d.	1055	623	5273	97	1488	2132
104	b.d.	b.d.	b.d.	b.d.	1884	b.d.	2890	b.d.
105	b.d.	41	b.d.	b.d.	1356	49	b.d.	138
106	25	115	74	b.d.	2111	111	4217	b.d.
107	207	277	120	b.d.	1129	b.d.	1363	130
110	241	713	236	114	10181	27	1358	b.d.
111	384	697	394	b.d.	4656	27	4314	b.d.
112	b.d.	35	b.d.	b.d.	2810	80	5439	b.d.
113	84	b.d.	2272	517	3353	555	8043	410
114	15	140	b.d.	87	1216	b.d.	1510	b.d.
115	13	125	b.d.	b.d.	1716	92	3045	b.d.
116	b.d.	b.d.	129	b.d.	4700	54	9389	b.d.
117	26	85	3599	757	4007	685	2284	b.d.
119	146	237	179	175	1351	b.d.	1114	b.d.
122	82	102	2512	1623	2728	630	2966	693
123	b.d.	37	b.d.	b.d.	554	35	4253	b.d.
124	21	b.d.	b.d.	71	8470	911	11,148	b.d.
127	52	76	1452	627	3968	1684	1686	b.d.
129	186	580	184	b.d.	4181	333	808	b.d.
130	b.d.	b.d.	1412	348	5516	561	2861	b.d.
131	b.d.	41	3329	620	2783	1228	663	b.d.

Catskill redbed (UNY 13).
b.d.–below detection limit, n.a–not analysed.

rutile thermometry might be the best tool for calculating peak temperatures for ultrahigh temperature granulites.

The Shawangunk and Catskill samples originate from clastic wedges which are fed by the detritus of the Taconian and Acadian orogens, respectively (see review of McLennan et al., 2001). For the pebbly sandstones of the Shawangunk, Yeakel (1962) proposed a proximal source region ca. 70 km to the SE. Both clastic wedges are characterized by a zircon fraction of predominantly Grenville age (ca. 0.9 to 1.3 Ga; Gray and Zeitler, 1997; McLennan et al., 2001). Basically two tectonic scenarios are possible to explain the zircon data: (1) Grenville-age continental

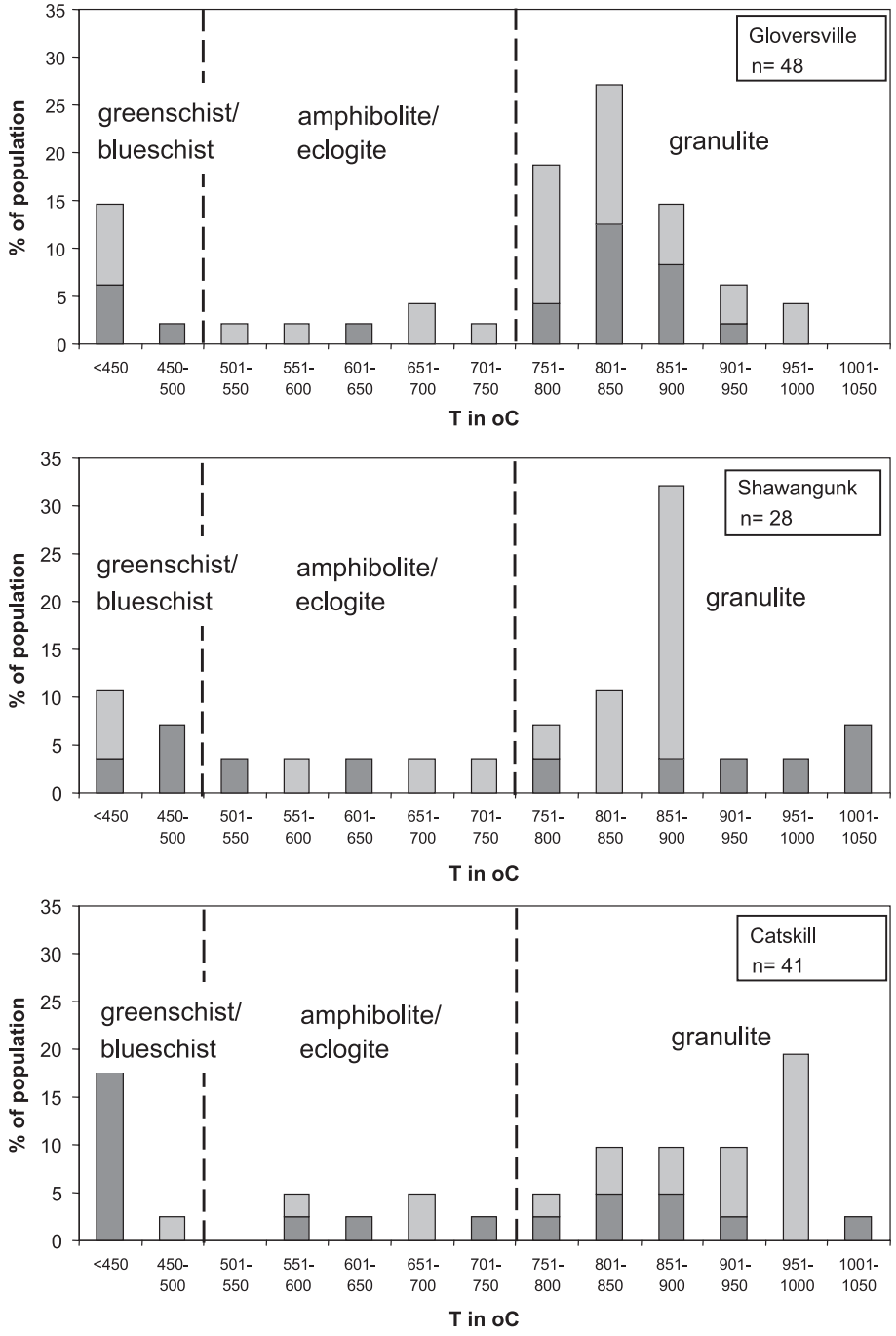

Fig. 6. Histogram of calculated metamorphic temperatures of metapelitic rutiles for Gloversville (UNY22), Shawangunk (UNY7) and Catskill samples (UNY13). Abundance in % of whole population. Dark grey: 63–125 μm size fraction, light grey: 125–250 μm size fraction. Approximate temperature regions of metamorphic facies are shown for comparison.

crust incorporated into the orogens is the source of the zircons (Gray and Zeitler, 1997). Rocks of such age are exposed today, e.g., in the Reading Prong and Piedmont crystalline provinces (Fig. 3). (2) Detritus from provenances of Grenville age were deposited in an accretionary prism and later recycled during the Taconian and Acadian orogenies (Bock et al., 1996; McLennan et al., 2001).

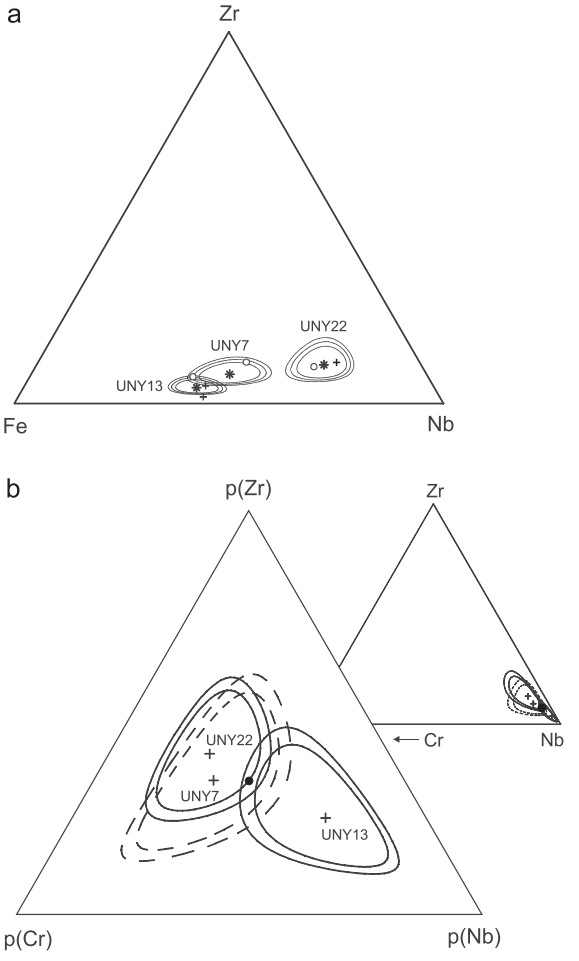

Fig. 7. (a) Rutile trace element composition illustrated in ternary diagram Zr–Fe–Nb. Stars indicate center (geometric mean) of each data set (sample), ellipsoids show confidence regions for the center with confidence limits of 80%, 90%, and 95% (see Weltje, 2002). Sample UNY22 can be separated from the others at 95% confidence limit. Open circles indicate center of rutiles from coarse fraction (125–250 μm), crosses indicate center of rutiles from fine fraction (63–125 μm). (b) Centered ternary diagram Zr–Cr–Nb (only fine fraction), that means the center of all the data (closed circle) is moved to the center of the diagram (see von Eynatten et al., 2002, for details of centering). Confidence regions have confidence limits of 80% and 90%. Stippled line belongs to sample UNY7. Small triangle shows position of confidence regions in a non-centered diagram. Sample UNY13 can be separated with ~80% confidence limit from samples UNY 7 and UNY 22.

Transferring the knowledge established for the detrital rutiles derived from the Adirondacks to the detrital rutiles from Shawangunk and Catskill reveals new facets of their provenance. One important result of this study is the discovery of abundant granulite-facies rutiles in both samples. Unlike zircon, rutile does not survive prograde metamorphism during greenschist and lower amphibolite facies. Therefore, detrital granulite-facies rutiles are either derived from granulites formed during the last metamorphic cycle or were recycled from (meta)sandstones that were fed by granulite-facies source rocks and did not undergo more than subgreenschist facies conditions after deposition.

From the above considerations, the tectonic scenario (1) is less likely. Although crystalline rocks from the Reading Prong and Piedmont crystalline provinces are of Grenville age, they experienced at least greenschist facies conditions during Taconian and Acadian orogeny, so that all rutile derived from this region must be newly crystallized and would not display such high proportions of granulite-facies rutiles as observed in samples UNY 7 and 13. Although granulite-facies conditions are found today in parts of the Piedmont (Wagner and Srogi, 1987), no indication of extreme temperatures (up to 1050 °C) has been found so far. Granulite-facies rocks are also rarely outcropping in active mountain belts (e.g., in the Alps granulite-facies rocks are regionally only found in a ca. 4 by 15 km area of the western Ivrea-Verbano Zone: Zingg, 1983) and it is more likely that deep levels of an orogen are exposed in old orogens. However, if a geochemical and -chronological study of rutile from the Reading Prong and Piedmont crystalline provinces yielded comparable results as detrital rutiles from Taconian and Acadian sediments, tectonic scenario (1) could be strengthened.

Instead, tectonic scenario (2) is consistent with the available zircon and rutile as well as with sedimentological data. In this scenario, both Grenville age zircons and granulite-facies rutiles are originally from the Grenville Province, having been deeply eroded by the end of the Precambrian so that granulite-facies rocks were extensively exposed. The zircon- and rutile-bearing detritus was deposited in an evolving

accretionary prism (Bock et al., 1996) that experienced only subgreenschist facies conditions, so that both zircon and rutile remained stable. In fact, accretionary prisms typically contain abundant quartz veins, which have been proposed to be the source of most of the Shawangunk quartz pebbles (Hemming, 1994). Evidence of this accretionary wedge is found today almost exclusively in the Taconian and Acadian clastic wedges, except possibly in a sequence of low grade metasedimentary and metavolcanic rocks found on the north border of the Reading Prong as stratigraphically high thrust sheets (the proposed source for Shawangunk sediments by Epstein and Epstein, 1972).

4. Implications for quantitative provenance studies

We have demonstrated that detrital rutile reveals a large chemical variety with respect to the incorporation of specific trace elements. These variations in rutile composition can be interpreted in terms of source rock lithology, as well as metamorphic peak temperature in the case of rutiles derived from metapelitic source rocks. In addition, rutile is extremely stable within sedimentary processes making it a very suitable mineral for provenance studies of both immature and mature sediments. In contrast to zircon, rutile is not stable at metamorphic conditions exceeding subgreenschist facies. Thus, provenance information derived from detrital rutile is generally related to the last medium to high-grade metamorphism, and has not undergone multiple recycling during orogenies.

Trace element systematics relating specific rutile compositions to specific host rocks allows for a direct linkage between the analysed detrital mineral composition and the source rock type from which it is derived. This is not trivial because most mineral compositions other than rutile largely depend on coexisting mineral phases, which are often unknown when dealing with sand-sized or even finer-grained sediments. The systematics of Nb and Cr are well understood, which permits the rutiles to be allotted between the metabasic and metapelitic host rocks. Furthermore, host rock types are expected to be distinguishable when analysing rutile from a broader variety of rocks. Beside source rock characterisation, such systematics may be useful for quantifying relative changes in the contribution of different source rocks to a depositional basin within time and/or space. If the absolute amount of rutile in two or even more source rocks within a drainage area can be estimated with some precision, the relative contribution of each of these source rocks to the total sediment derived from that drainage area can be calculated.

Calculating metamorphic peak temperatures from detrital rutiles provides additional geothermometric information on the source rocks. Therefore, tracing detrital rutile composition through time within the sedimentary record simultaneously elucidates the geodynamic history of the source area, e.g., the exhumation of metamorphic cores where rocks with gradually increasing metamorphic peak temperatures are exposed to the surface. Cooling rates of the source rocks may then be calculated by dividing the incremental increase in metamorphic peak temperature by the difference between the chronostratigraphic ages of the rutile-bearing sediments. With regard to the potential of rutile dating by newly developed techniques (see above), calculating cooling rates from detrital rutile and thus constraining the related geodynamic processes appears to be a very promising tool for forthcoming quantitative provenance analysis.

In a final note, the ratio between the hydrologically similar minerals zircon and rutile (Morton and Hallsworth, 1994) appears to be useful in further quantifying contributions from different source rocks. Zircon is an omnipresent accessory mineral in most magmatic (e.g., granites) and metamorphic rocks, while rutile is restricted to certain metamorphic rocks. However, if present, rutile is more abundant than zircon (~1 vs. ~0.01 modal%, respectively), so that zircon/rutile-ratios can differ from $\gg 10$ in sediments derived from granites to <1 in sediments derived from metapelitic rocks. Our data show that one sediment sample from a local source with a high ratio of metapelites to granites gives a relatively low zircon/rutile-ratio of 3 (Gloversville sample), while mature sediments from different sources give a zircon/rutile-ratio of 9 (Shawangunk and Catskill samples).

5. Conclusion

Based on the trace element systematics known to date, the recently developed Zr-in-rutile geothermometer as well as the encouraging results from the case

study of sediments of Upstate New York, the following conclusions are drawn concerning the potential of rutile geochemistry for quantitative provenance analysis:

(i) detrital rutile displays a large variation in trace element composition suggesting a high potential for discrimination of rutiles derived from different source rocks or source areas,
(ii) in contrast to zircon, rutile is not stable within metamorphic processes exceeding subgreenschist facies conditions. Therefore, provenance information derived from detrital rutile is much less biased by the possibility of multiple recycling within the rock cycle, e.g., during orogeny,
(iii) beyond source rock characterisation, rutile trace element systematics may allow for quantifying the relative contribution of different source rocks to the total sediment derived from a specific source area, and
(iv) the calculation of metamorphic peak temperatures from detrital rutiles provides geothermometric information on source rocks, and thus allows for tracing geodynamic processes in the source area, e.g., the exhumation of metamorphic cores.

Acknowledgement

We would like to express our sincere thanks to Ann Ewing for help during the initial stages of this work. Frank Linde and Lena Schilling are thanked for help in the laboratory. We appreciate fruitful discussions with and help from Barbara Bock, Sidney Hemming, Diane McDaniel and Roberta Rudnick. Financial support is acknowledged from Deutsche Forschungsgemeinschaft (ZA 285/2, EY 23/3), the Forschungspool of Universität Heidelberg, NSF (REU fund) and the University of Maryland. We appreciate constructive reviews by Andy Morton and Conny Spiegel.

References

Alcock, J., Muller, P.D., 1999. Very high-temperature, moderate-pressure metamorphism in the New Russia gneiss complex, northeastern Adirondack Highlands, metamorphic aureole to the Marcy anorthosite. Can. J. Earth Sci. 36, 1–13.

Barth, M.G., McDonough, W.F., Rudnick, R.L., 2000. Tracking the budget of Nb and Ta in the continental crust. Chem. Geol. 165, 197–213.

Bock, B., McLennan, S.M., Hanson, G.N., 1996. The Taconian orogeny in southern New England: Nd-isotope evidence against addition of juvenile components. Can. J. Earth Sci. 33, 1612–1627.

Bohlen, S.R., Valley, J.W., Essene, E.J., 1985. Metamorphism in the adirondacks: I. Petrology, pressure and temperature. J. Petrol. 26, 971–992.

Carter, A., Bristow, C.S., 2003. Linking hinterland evolution and continental basin sedimentation by using detrital zircon thermochronology: a study of the Khorat Plateau Basin, eastern Thailand. Basin Res. 15, 271–285.

Crowhurst, P., Farley, K., Ryan, C., Duddy, I., Blacklock, K., 2002. Potential of rutile as a U–Th–He thermochronometer. Eleventh Annual Goldschmidt Conference, LPI Contribution 1088 (CD-Rom), Lunar and Planetary Institute, Houston, TX, 2001, pp. 158.

Deer, W.A., Howie, R.A., Zussmann, J., 1962. Rock-forming minerals, v. 5, Non-silicates. Longmans. 371 pp.

Deer, W.A., Howie, R.A., Zussmann, J., 1992. An introduction to rock-forming minerals. Longmans Scientific and Technical. 696 pp.

Dineen, R.J., Hanson, E., 1995. Glacial deposits in the Mohawk and Sacandaga valleys or a tale of two tongues redux. In: Garver, J.I., Smith, J.A. (Eds.), Field trips for the 67th annual meeting of the New York State Geological Association Union College, Schenectady, pp. 39–55.

Epstein, J.B., Epstein, A.G., 1972. The shawangunk formation (upper Ordovician (?) to middle Silurian) in eastern Pennsylvania. U.S. Geol. Surv. Prof. Pap. 774, 1–45.

Faupl, P., Petrakakis, K., Migiros, G., Pavlopoulos, A., 2002. Detrital blue amphibole from the western Othrys Mountain and their relationship to the blueschist terrains of the Hellenides (Greece). Int. J. Earth Sci. 91, 433–444.

Force, E.R., 1980. The provenance of rutile. J. Sediment. Petrol. 50, 485–488.

Force, E.R., 1991. Geology of titanium-mineral deposits. Geological Society of America Special Paper vol. 259. Boulder, 112 pp.

Götze, J., 1996. Genetic information of accessory minerals in clastic sediments. Zentralbl. Geol. Palaontol., Teil 1 1995, 101–118.

Graham, J., Morris, R.C., 1973. Tungsten- and antimony-substituted rutile. Min. Mag. 39, 470–473.

Gray, M.B., Zeitler, P.K., 1997. Comparison of clastic wedge provenance in the Appalachian foreland using U/Pb ages of detrital zircon. Tectonics 16, 151–160.

Haggerty, S.E., 1991. Oxide mineralogy of the upper mantle. In: Lindsley, D.H. (Ed.), Oxide Minerals: Petrological and Magnetic Significance, Rev. Miner. vol. 25. , pp. 355–416.

Harley, S.L., 1989. The origin of granulites: a metamorphic perspective. Geol. Mag. 126, 215–247.

Hemming, S.R., 1994. Pb isotope studies of sedimentary rocks and detrital components for provenance analysis. PhD dissertation. State University of New York at Stony Brook, 212 pp.

Hubert, J.F., 1962. A zircon–tourmaline–rutile maturity index and the interdependance of the composition of heavy mineral

assemblages with the gross composition and texture of sandstones. J. Sediment. Petrol. 32, 440–450.
Jacobsen, Y.J., Münker, C., Mezger, K., 2003. Hf isotope compositions in detrital zircons as a new tool for provenance studies. Geophys. Res. Abstr. 5, 10282.
Kesler, S.E., Friedman, G.M., Krstic, D., 1997. Mississippi Valley-type mineralization in the Silurian paleoaquifer, central Appalachians. Chem. Geol. 138, 127–134.
LaTourrette, T., Hervig, R.L., Holloway, J.R., 1995. Trace element partitioning between amphibole, phlogopite, and basanite melt. Earth Planet. Sci. Let. 135, 13–30.
Mange, M.A., Maurer, H.F.W., 1992. Heavy Minerals in Colour. Chapman and Hall, London. 148 pp.
McLennan, S., Bock, B., Compston, W., Hemming, S., McDaniel, D., 2001. Detrital zircon geochronology of Taconian and Acadian foreland sedimentary rocks in New England. J. Sediment. Res. 71, 305–317.
Morton, A.C., 1987. Influences of provenance and diagenesis on detrital garnet suites in the Forties sandstone, Paleocene, central North Sea. J. Sediment. Petrol. 57, 1027–1032.
Morton, A.C., Hallsworth, C., 1994. Identifying provenance-specific features of detrital heavy mineral assemblages in sandstones. Sediment. Geol. 90, 241–256.
Morton, A.C., Hallsworth, C., 1999. Processes controlling the composition of heavy mineral assemblages in sandstones. Sediment. Geol. 124, 3–29.
Pattison, D.R.M., Chacko, T., Farquhar, J., McFarlane, C.R.M., 2003. Temperatures of granulite-facies metamorphism: constraints from experimental phase equilibria and thermobarometry corrected for retrograde exchange. J. Petrol. 44, 867–900.
Plank, T., Langmuir, C.H., 1998. The chemical composition of subducting sediment and its consequences for the crust and mantle. Chem. Geol. 145, 325–394.
Pober, E., Faupl, P., 1988. The chemistry of detrital chromian spinels and its implications for the geodynamic evolution of the Eastern Alps. Geol. Rundsch. 77, 641–670.
Preston, J., Hartley, A., Hole, M., Buck, S., Bond, J., Mange, M., Still, J., 1998. Integrated whole-rock trace element geochemistry and heavy mineral chemistry studies: aids to the correlation of continental red-bed reservoir in the Beryl Field, UK North Sea. Pet. Geosci. 4, 7–16.
Preston, J., Hartley, A., Mange-Rajetzky, M., Hole, M., May, G., Buck, S., Vaughan, L., 2002. The provenance of Triassic continental sandstones from the Beryl field, northern North Sea: mineralogical, geochemical, and sedimentological constraints. J. Sediment. Res. 72, 18–29.
Rahl, J.M., Reiners, P.W., Campbell, I.H., Nicolescu, S., Allen, C.M., 2003. Combined single-grain (U–Th)/He and U/Pb dating of detrital zircons from the Navajo Sandstone, Utah. Geology 31, 761–764.
Rice, C.M., Darke, K.E., Still, J.W., 1998. Tungsten-bearing rutile from the Kori Kollo gold mine, Bolivia. Mineral. Mag. 62, 421–429.
Sircombe, K.N, 1996. Provenance of heavy detritical minerals in coastal sands and sedimentary rocks of Eastern Australia using the SHRIMP ion probe. Abstr. with programs. Geol. Soc. Am. 28 (7), 279.
Smith, D.C., Perseil, E.A., 1997. Sb-rich rutile in the manganese concentrations at St. Marcel-Praborna, Aosta Valley, Italy: petrology and crystal-chemistry. Mineral. Mag. 61, 655–669.
Spear, F.S., Markussen, J.C., 1997. Mineral zoning, P-T-X-M phase relations, and metamorphic evolution of some Adirondack Granulites, New York. J. Petrol. 38, 757–783.
Spiegel, C., Siebel, W., Frisch, W., Zsolt, B., 2002. Nd and Sr isotopic ratios and trace element geochemistry of epidote from the Swiss Molasse Basin as provenance indicators: implications for the reconstruction of the exhumation history of the Central Alps. Chem. Geol. 189, 231–250.
von Eynatten, H., 2003. Petrography and chemistry of sandstones from the Swiss Molasse Basin: an archive of the Oligocene to Miocene evolution of the Central Alps. Sedimentology 50, 703–724.
von Eynatten, H., Gaupp, R., 1999. Provenance of Cretaceous synorogenic sandstones in the Eastern Alps: constraints from framework petrography, heavy mineral analysis, and mineral chemistry. Sediment. Geol. 124, 81–111.
von Eynatten, H., Wijbrans, J.R., 2003. Precise tracing of exhumation and provenance using Ar/Ar-geochronology of detrital white mica: the example of the Central Alps. Spec. Publ.-Geol. Soc. London 208, 289–305.
von Eynatten, H., Gaupp, R., Wijbrans, J.R., 1996. 40Ar/39Ar laser-probe dating of detrital white micas from Cretaceous sedimentary rocks of the Eastern Alps: Evidence for Variscan high-pressure metamorphism and implications for Alpine orogeny. Geology 24, 691–694.
von Eynatten, H., Pawlowsky-Glahn, V., Egozcue, J.J., 2002. Understanding perturbation on the simplex: a simple method to better visualise and interpret compositional data in ternary diagrams. Math. Geol. 34, 249–257.
Wagner, M.E., Srogi, L., 1987. Early Paleozoic metamorphism at two structural levels and a model for the Pennsylvania–Delaware Piedmont. Bull. Geol. Soc. Am. 99, 113–126.
Weltje, G.J., 2002. Quantitative analysis of detrital modes: statistically rigorous confidence regions in ternary diagrams and their use in sedimentary petrology. Earth-Sci. Rev. 57, 211–253.
Yeakel Jr, L.S., 1962. Tuscarora, Juniata, and Bald Eagle paleocurrents in the central Appalachians. Bull. Geol. Soc. Am. 73, 1515–1540.
Zack, T., Kronz, A., Foley, S., Rivers, T., 2002. Trace element abundances in rutiles from eclogites and associated garnet mica schists. Chem. Geol. 184, 97–122.
Zack, T., Moraes, R., Kronz, A., in preparation. Temperature-dependence of Zr in rutile: empirical calibration of a rutile thermometer. Contr. Min. Petrol., in press.
Zingg, A., 1983. The Ivrea and Strona-Ceneri Zones (Southern Alps, Ticino and N-Italy)—a review. Schweiz. Mineral. Petrogr. Mitt. 63, 361–392.